Model-Based Parametric Inversion of Controlled Source Electromagnetic Data in Two and Half Dimensions

Maokun Li[1], Aria Abubakar[1], Tarek M. Habashy[1]

[1]Schlumberger-Doll Research, Cambridge, MA 02139, USA, (email: aabubakar@slb.com)

Abstract

A model-based parametric inversion method will be introduced in this communication for the reconstruction of regions of interests including their conductivities and shapes. It is applied to marine controlled-source electromagnetic data. By incorporating the priori information acquired from seismic or gravity measurements or pixel-based inversion method, this scheme can approximate parameters with a less unknown number in the inversion process. It is based on a general Gauss-Newton minimization framework with several techniques set up to ensure a stable convergence, such as constraint minimization, quadratic line search, and etc. By doing this, this algorithm is shown to be accurate and efficient.

1.Introduction

With the rapid development of sensor technologies as well as computer and signal processing algorithms, the marine controlled-source electromagnetic (CSEM) technology has recently gained significant attention for off-shore oil exploration. With a horizontal electric dipole transmitting very low frequency electromagnetic waves (0.1~10 Hz) towed by a ship and multi-component electromagnetic receivers on the seafloor, this method has recently been successful in several field surveys. In physics, the electromagnetic wave couples more to the sea bed due to the large conductivity of the sea water. Moreover, the high contrast in resistivity between saline-filled rocks and hydrocarbons makes this method well suited for detecting thin oil reservoirs. It has been described by some researchers as "may well become the most important geophysical technique to emerge since the advent of 3D reflection seismology" [1].

In the interpretation of CSEM data, nonlinear inversion algorithms are more attractive because of its accuracy for high-contrast regions. A common way in the inversion process is to divide the domain of interest into subgrids with unknowns parameters defined on each pixel, and then apply an optimization approach to match the responses between the data observed and the data generated from the estimated model. Several inversion algorithms have been proposed such as [2, 3] to predict the conductivity distributions. The list here is far from complete due to space limitations.

In this abstract, we present a model-based inversion scheme for processing the CSEM data, which reconstructs the conductivities and shapes of the regions of interest based on some *a priori* information. The required *a priori* information can come from independent measurements (e.g., seismic) or from the inversion results of the same data using a pixel-based inversion approach [2]. The model-based inversion presented in this paper, generalizes the so-called sharp boundary inversion approach [4, 5]. This model-based inversion scheme is based on a Gauss-Newton minimization method with multiplicative regularization and a line search approach to stabilize the inversion process [6]. The forward solver is based on a two-and-half dimensional frequency domain finite-difference simulator described in [2]. In this model-based inversion algorithm, the shape of the various regions, expressed as two dimensional (2D) polygons defined by their vertices, can be reconstructed along with their locations and conductivities. Some initial numerical tests of CSEM models show good reconstructions.

2. Formulations

2.1 Geometry Models

Figure 1 shows an example of the geometry setup in two dimensions. Each region with a different conductivity is modeled with a polygon described by the coordinates (x, z) of its vertices. Cubic spline interpolation is used to define the polygon boundaries except sharp corners. Therefore, the conductivity distribution can be written as $f(x, z, \sigma_r, \overline{\mathbf{x}}_r, \overline{\mathbf{z}}_r)$, where x and z indicate the coordinates of the points in the inversion domain, $\overline{\mathbf{x}}_r$ and $\overline{\mathbf{z}}_r$ indicate the vertices of the polygons, and σ_r is the conductivity of the region

inside the polygon. The number of vertices depends on the complexity of the geometry. Furthermore, other model parameters can also be used, such as the centroids of the regions.

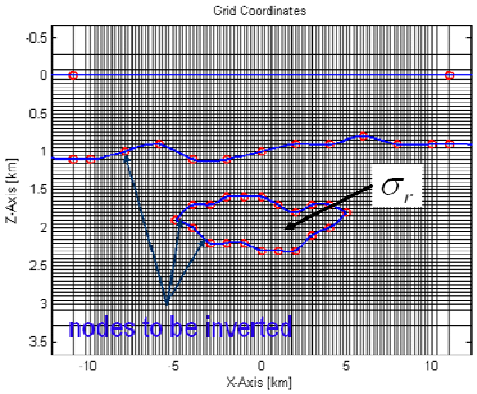

Figure 1: An example of geometry model in the simulation. The red circle indicates the nodes to be inverted for their coordinates.

2.2 Forward Algorithm

The forward solver used a frequency domain finite difference algorithm [2] to solve the Maxwell equations for electric field. In order to render the forward algorithm more efficient, several techniques have been applied. For example, the regions outside the domain of interest are discretized using optimal grids in both x and z directions. This helps to reduce the number of unknowns while still maintaining a good accuracy [8]. This optimal grid technique is also used to select the spatial frequency components along the invariant y-direction. Moreover, a material averaging formula [9] is used to calculate the effective material properties on both small and large grids. Finally, since the matrix generated from the finite-difference method is very sparse, a multi-frontal LU decomposition method is used as the solver, which can be very efficient for solving the electric field equation with multiple right-hand sides.

2.3 Inversion Algorithm

The inversion algorithms based on a regularized Gauss-Newton method [6]. The cost function for optimization is defined as follows:

$$C_k(\bar{\mathbf{m}}) = \frac{1}{2}\left\|\overline{\overline{\mathbf{W}}}_d \cdot \bar{\mathbf{e}}(\bar{\mathbf{m}})\right\|^2 + \frac{1}{2}\lambda_k \left\|\overline{\overline{\mathbf{W}}}_x \cdot (\bar{\mathbf{m}} - \bar{\mathbf{m}}_k)\right\|^2, \tag{1}$$

where $\bar{\mathbf{m}}$ is the vector of model parameters that includes the coordinates of vertices and centers of the polygonal regions as well as the conductivities. $\bar{\mathbf{e}}(\bar{\mathbf{m}})$ is the vector of data misfit expressed as $\bar{\mathbf{e}}(\bar{\mathbf{m}}) = (\bar{\mathbf{S}}(\bar{\mathbf{m}}) - \mathbf{d}) / \left\|\bar{\mathbf{d}}\right\|$, where $\bar{\mathbf{S}}(\bar{\mathbf{m}})$ is a vector containing the simulated data from the model and $\bar{\mathbf{d}}$ is the vector of the measured data. $\overline{\overline{\mathbf{W}}}_d$ and $\overline{\overline{\mathbf{W}}}_m$ are weighting matrices that put the various data on equal footing. λ_k is the regularization parameter at the kth iteration. A multiplicative regularization scheme is used to link the regularization factor λ_k to the data misfit at the kth iteration as $\lambda_k = \left\|\overline{\overline{\mathbf{W}}}_d \cdot \bar{\mathbf{e}}(\bar{\mathbf{m}})\right\| / 2\delta^2$ where δ is a constant determined by numerical trials. This scheme can adaptively adjust the impact of regularization on the cost function hence is more robust relative to the traditional additive regularization scheme.

2.4 Constraint Minimizations

Constrained minimization is important in this model-based inversion algorithm to guarantee the reconstructed shapes physically realistic. It will also help to reduce the non-uniqueness in estimating other parameters such as the center locations and conductivities. In the current algorithm, the maximum and minimum values of conductivity are decided from geological considerations and the centers are constrained to be within the region of inversion. Furthermore, the vertices of the polygons are constrained to $[-ar_{\min}, ar_{\min}]$ where $r_{\min}$ is the minimum distance from the node to all other nodes of the polygon, and $a \in (0, 1/2]$ is a constant that scales the step length in different directions. A nonlinear transformation is used to constrain the various model parameters and is given generically by:

$$m = m_{\min} + \frac{m_{\max} - m_{\min}}{c^2 + 1} c^2 , \tag{2}$$

where $c \in (-\infty, \infty)$ is an auxiliary inversion parameter that transforms the constrained minimization problem to an unconstrained one. The search step, q, for the parameter c is related to the step p of m as follows:

$$q = \frac{\partial c}{\partial m} p = \frac{1}{2} \frac{m_{\max} - m_{\min}}{m_{\max} - m} \sqrt{(m - m_{\min})(m_{\max} - m)}\, p . \tag{3}$$

Therefore the update of m can be written explicitly as

$$m_{k+1} = m_k + \frac{m_{\max} - m_{\min}}{\alpha_k^2 + (m_k - m_{\min})(m_{\max} - m_k)^3} \alpha_k^2 , \tag{4}$$

and $\alpha_k = (m_k - m_{min})(m_{max} - m_k) + (m_{max} - m_{min}) \nu_k p_k$, while ν_k is computed using a line search algorithm that guarantees a reduction of the cost function at each iteration [6].

2.5 Jacobian Matrix

The Jacobian matrix is computed from a chain-rule as

$$J_{q,r} = \frac{\partial S_q}{\partial m_r} = \sum_{k,l} \frac{\partial S_q}{\partial \sigma_{k,l}} \frac{\partial \sigma_{k,l}}{\partial m_r} , \tag{5}$$

where $\partial S_q / \partial \sigma_{k,l}$ is the Jacobian with respect to the conductivity of pixel (k, l), which is computed using an adjoint approach, and $\partial \sigma_{k,l} / \partial m_r$ is the derivative of the pixel conductivity with respect to the model parameter m_r. The latter is obtained using a finite-difference approximation as $\partial \sigma_{k,l} / \partial m_r \approx \left(\tilde{\sigma}_{k,l}(m_r + \delta m_r) - \tilde{\sigma}_{k,l}(m_r) \right) / \delta m_r$. $\tilde{\sigma}$ indicates the effective conductivity of a cell after material averaging and is given by:

$$\tilde{\sigma}_{k,l}(m_r) = \left\{ \sum_{l'} \left(\sum_{k'} \tilde{\sigma}_{k,l;k',l'}(m_r) \right)^{-1} \right\}^{-1/2} \times \left\{ \sum_{k'} \left(\sum_{l'} \tilde{\sigma}_{k,l;k',l'}(m_r) \right)^{-1} \right\}^{-1/2} \tag{6}$$

with k' and l' denoting the indices of sub-pixels.

3. Numerical Examples

Figure 2 shows an example of inverting high resistivity regions from synthetic CSEM data. Two thin resistivity regions are embedded in the seabed at different levels with conductivities 0.075 S/m (lower one) and 0.05 S/m (upper one). Figure 2(a) shows the model used to generate the data. There are 21 receivers at the sea bottom with 1 km intervals and 41 sources located 50 m above with 0.5 km intervals. The operating frequency is 0.25 Hz. The computational domain is discretized into 120 × 80 cells, where the inner 100 × 60 cells are regular grids and the outer ones are non-uniform using the optimal grid approach. Parameters including centroids and conductivities of the two regions, as well as the coordinates of their vertices, will be optimized according to the data recorded by the receivers. Figure 2(b) shows the initial guess of the model, with a conductivity of 0.1 S/m in both regions. The inversion result after 35 iterations is shown in Figure 2(c). Its difference with the original model is shown in Fig. 2(d). We can see a good agreement between the reconstructed and the true model with a maximum error in conductivity of 8%.

4. Conclusion

A model-based parametric inversion algorithm is developed for the interpretation of CSEM data. The model parameters, such as the conductivities, the positions of the centroids and vertices of the polygons, are successfully inverted from the measurement data based on some initial guess. The attractive feature of this inversion approach is that the number of unknowns to be inverted for is much smaller than for the pixel-based inversion method, hence it is more efficient and fast.

5. Acknowledgments

The authors thank V. Druskin of Schlumberger-Doll Research, Cambridge, MA, USA and L. Knizhnerman of the Center for Geophysical Expedition, Moscow, Russia for providing the 2.5D finite-difference forward program.

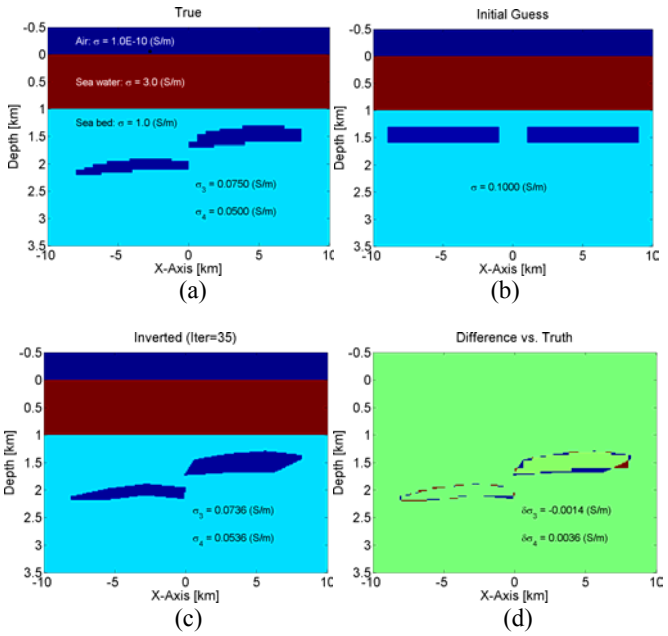

Figure 2: An example of inversion of multiple objects with synthetic data.

6. References

1. S. Constable and L. J. Srnka, "An introduction to marine controlled-source electromagnetic methods for hydrocarbon exploration," *Geophysics,* 72(2), 2007, pp. WA3-WA12.

2. A. Abubakar, T. Habashy, V. Druskin, D. Alumbaugh, A. Zerelli, and L. Knizhnerman, "Two-and-half-dimensional forward and inverse modeling for marine CSEM problems," in *SEG technical program expanded abstracts*, vol. 25, New Orleans, LA, 2006, pp. 750-754.

3. A. Gribenko, and M. Zhdanov, Rigorous 3d inversion of marine csem data based on the integral equation method. *Geophysics*, 72(2), 2007, pp. WA73-WA84.

4. T. Smith, M. Hoversten, E. Gasperikova, and F. Morrison, "Sharp boundary inversion of 2D magnetotelluric data," *Geophysical Prospecting*, 47(4), 1999, pp. 469-486.

5. G. M. Hoversten, T. Rosten, K. Hokstad, D. Alumbaugh, S. Horne, and G. A. Newman, "Integration of multiple electromagnetic imaging and inversion techniques for prospect evaluation," in *SEG technical program expanded abstracts*, vol. 25, New Orleans, LA, 2006, pp. 719-723.

6. T. M. Habashy, and A. Abubakar, "A general framework for constraint minimization for the inversion of electromagnetic measurements," *Progress in Electromagnetics Research*, 46, 2004, pp. 265-312.

7. K. Yee, "Numerical solution of inital boundary value problems involving maxwell's equations in isotropic media", *IEEE Trans. Antennas Propagat.*, vol. 14(3), 1966, pp. 302-307.

8. D. Ingerman, V. Druskin, and L. Knizhnerman, "Optimal finite difference grids and rational approximations of the square root I. Elliptic problems," *Comm. Pure. Appl. Math.*, vol. 53(8), 2000, pp. 1039-1066.

9. J. B. Keller, "A theorem on the conductivity of a composite medium," *J. Math. Phys.*, vol. 5(4), 1964, pp. 548-549.